



Human disturbance on phosphorus sources, processes and riverine export in a subtropical watershed



Xin Yuan ^{a,b}, Michael D. Krom ^{c,d}, Mingzhen Zhang ^{a,b}, Nengwang Chen ^{a,b,*}

^a Fujian Provincial Key Laboratory for Coastal Ecology and Environmental Studies, College of the Environment and Ecology, Xiamen University, Xiamen 361102, China

^b Key Laboratory of the Coastal and Wetland Ecosystems, College of the Environment and Ecology, Xiamen University, Xiamen 361102, China

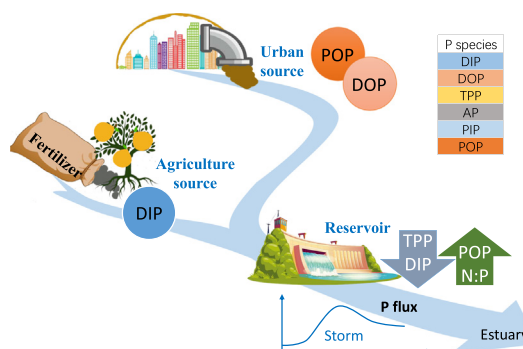
^c Morris Kahn Marine Research Station, Department of Marine Biology, Leon H. Charney School of Marine Science, University of Haifa, Haifa 3498838, Israel

^d School of Earth and Environment, University of Leeds, Leeds LS2 9JT, UK

HIGHLIGHTS

- Agriculture and urban pollution sources were characterized for their P speciation.
- More total (and organic) P was carried down the North river during the wet season.
- Reservoirs decrease particulate P and phosphate but increase dissolved organic P.
- Storms induced a disproportionately high fraction of P flux down the river system.
- The high N:P ratio in the river confirms the key role of P in eutrophication.

GRAPHICAL ABSTRACT



ARTICLE INFO

Article history:

Received 22 October 2020

Received in revised form 13 December 2020

Accepted 16 December 2020

Available online 19 January 2021

Editor: Fernando A.L. Pacheco

Keywords:

Pollution sources

Reservoirs

Land use

Climate change

Jiulong River

ABSTRACT

Phosphorus (P) is a key nutrient in freshwater systems, often acting as the limiting nutrient. The dominant sources of P in the Jiulong River watershed (S.E. China) are anthropogenic. Dissolved and particulate P species were measured in the West (WJR) and North (NJR) rivers during the wet and dry seasons of 2018 and at their river outlets during a storm (June 2019). Sources of P pollution were characterized from mainly single source subcatchments (dry season). The Agriculture source (WJR) had a total P of $114.7 \pm 13.1 \mu\text{g P L}^{-1}$, which was mainly dissolved inorganic P (DIP) from excess fertilizer washed from the fields. By contrast, the West Urban source (sewage effluent) was mainly particulate (POP) and dissolved organic P (DOP). The effect of reservoirs in the main NJR was to decrease total particulate P (TPP) and DIP and increase POP, due to increased sedimentation of particles and biological uptake. An increase in all P species was observed at the beginning of the storm, followed by a decrease on the rising hydrograph due to dilution. The final concentration of all P species was higher than baseflow, confirming that storms increase the P flux out of the watershed. P was initially washed off the fields during the storm, and during the falling hydrograph P increased due to interflow and other longer-term sources. The high DIN:DIP ratio confirmed the key importance of P inputs from human activities in substantially altering P sources and cycling, and hence the importance of science-based management to alleviate the eutrophication problem.

© 2021 Elsevier B.V. All rights reserved.

* Corresponding author at: College of the Environment and Ecology, Xiamen University, Xiamen, Fujian 361102, China.

E-mail address: nwchen@xmu.edu.cn (N. Chen).

1. Introduction

Phosphorus (P) is an important nutrient in aquatic ecosystems. In freshwater ecosystems it is commonly the limiting nutrient controlling primary productivity, and determining the total biomass of algal organisms (Elser, 2012; Kang et al., 2017). Although P is supplied to river systems by natural weathering of rocks and soils in the catchment, in most modern rivers (including the Jiulong River in S.E. China, the subject of this study) the dominant source of P is anthropogenic pollution (Filippelli, 2008). Phosphorus is a major component of agricultural fertilizers and mostly reaches rivers via surface runoff during major rainfall events, but is also discharged into rivers in domestic and agricultural waste effluent (Van Drecht et al., 2009). As the amount of P pollution increases there is generally a non-linear response by the river ecosystem; the early increase in P content causes a linear increase in biomass and diversity of the still healthy ecosystem, but continuing excessive P input will cause eutrophication of surface water which will negatively affect water quality in the river system (Tilman, 1999). The impacts include the weakening of aquatic ecosystem function, loss of biodiversity, and decline in water quality which can result in areas of hypoxia. Harmful algal blooms associated with eutrophication can produce toxic algae which can kill aquatic animals, and occasionally even have harmful effects on humans (Lenes et al., 2008; Niyogi et al., 2007; Reinhard et al., 2017; Schoumans et al., 2014).

River systems represent the most important channel for the transportation of land P into the ocean. Globally 75%–94% of P inputs to the coastal and hence oceanic systems is via rivers, with the total P flux transported by global rivers to coastal areas being about $17.5\text{--}21.0 \times 10^9 \text{ kg y}^{-1}$ (Benitez-Nelson, 2000; Treguer et al., 1995; Wei et al., 2011). This input of dissolved and particulate P to river systems and from there exported to coastal regions is mainly regulated by human activities and hydrological conditions and no longer by natural weathering processes (River and Richardson, 2018; Zimmer and Lautz, 2014). With the increase in population and economic development (especially intensive agriculture and the acceleration of urbanization and industrialization), the impact of human activities on P output in river basins is likely to increase further (Seitzinger et al., 2010).

The Jiulong River is a typical subtropical river in China, and as with many such rivers there is a complex variety of different sources of P into the river. Phosphorus concentrations in the Jiulong River system have obvious spatial and seasonal differences. The Jiulong River watershed has a semi-tropical climate and a clear wet and dry season. The summer monsoonal season has both higher rainfall and higher plant growth compared to the somewhat drier winter season. In addition to these seasonal changes there are occasional major storms; these periods of high rainfall result in nutrients (N and P) being flushed from the catchment into the river and increasing the flux, though not necessarily the concentration, of these pollutants downstream (Gao et al., 2018). The mean concentration of total P (TP) in storm runoff from agricultural watersheds is generally higher than in urbanized watersheds, and both are higher than natural or even cultivated forests (Chen et al., 2015). However, our understanding of the contributions of different sections of the river to specific P forms is still limited.

Dams and their reservoirs increase hydraulic retention time and thus modify both the nature and amount of P exported downstream (Lu et al., 2016; Maavara et al., 2015; Maavara et al., 2020). On the one hand, there is increased algal uptake of P in the less dynamic water retained behind dams, often as algal blooms, and some of this particulate organic P is released downstream of the dam. On the other hand, the reservoirs behind the dams are locations where particulate matter, including autochthonic algae and P adsorbed onto particles, tend to settle and deposit. The resulting P-rich sediments represent a long-term store of potentially bioavailable P and some fraction can later be released into the water column, including via resuspension during large storm flow (Dynesius and Nilsson, 1994; Withers and Jarvie, 2008).

In addition to the various biogeochemical processes affecting environmental change in river systems in tropical and subtropical regions, there is the additional effect of climate change. It is now clear that one effect of climate change in these regions is an increase in extreme weather events such as storms and droughts, which will become more severe and frequent (Eccles et al., 2019). These events in turn affect the total P flux and its speciation into the river and from the river into the coastal system (Chen et al., 2015; Paerl, 2006).

The expansion of urbanization and rapid local economic development (particularly intensive agriculture in the watershed) will generate more P-rich anthropogenic waste, including sewage and agricultural discharges which will increase P flux into and through the watershed (Van Drecht et al., 2009). As a result, the Jiulong River ecosystem will require stricter environmental management to control the effects of increased eutrophication on ecosystem functions and deterioration of water quality (part of which is used as domestic water sources), and to reduce harmful effects on the adjacent Xiamen coastal system (N. Chen et al., 2018). A better understanding of the P sources and various biogeochemical processes occurred in the different sections of the river is essential to produce better science-based management decisions to achieve a more sustainable river ecosystem.

In this study we determined P species changes along the Jiulong River system, including adsorbed phosphorus (AP), particulate inorganic phosphorus (PIP), particulate organic phosphorus (POP), total particulate P (TPP), dissolved inorganic phosphorus (DIP), dissolved organic phosphorus (DOP), and dissolved total P (DTP) during the wet season and dry season in 2018. The aim was to identify major sources of P pollution into the river and their P characteristics by identifying sub-catchments with a single dominant source of P pollutant inputs. By following the changes down the river during the wet and dry seasons, we can summarize the main biogeochemical processes affecting P in different river sections. We also conducted detailed sampling during a storm in the summer of 2019 and used the changes in P speciation with discharge to identify important P sources which were flushed out of the system at these times of increased water flow. Finally, we determined the P flux from the river system to the head of the estuary and discussed how this varies between wet and dry seasons and affected by individual storms.

2. Materials and methods

2.1. Description of study site

The Jiulong River Watershed is located in S.E. China and has a catchment area of $1.47 \times 10^4 \text{ km}^2$ (Fig. 1). Typically the combined freshwater export to the coast of the two main tributaries is $1.24 \times 10^{10} \text{ m}^3 \text{ y}^{-1}$; the North Jiulong River (NJR) exports about two-thirds of this discharge and the West Jiulong River (WJR) exports one-third (Y.N. Chen et al., 2018). In the study year (2018) the annual discharge was reduced to $7.2 \times 10^9 \text{ m}^3 \text{ y}^{-1}$. The North River and West River have lengths of 274 km and 172 km, and drainage areas of 9640 km² and 3940 km², respectively. The watershed is within the Asian monsoon climate belt with the wet season from April to September (when 58% of rainfall occurred in 2018) and October to March comprising the dry season.

The upper reaches of the West River are dominated by intensive Pomelo orchards which receive heavy applications of inorganic fertilizers and manure. Downstream of these orchards, the main river channel and its three tributaries pass through land with more mixed agriculture, as well as towns and villages which discharge domestic and some industrial waste into the river system. The lowest reaches of the river receive agricultural runoff from crop lands and finally pass through Zhangzhou City (population 0.8 million), which discharges its treated and raw domestic waste into the river. The North River is longer and has a higher flow. The upper reaches of the NJR flow past Longyan City (population 0.7 million) to Zhangping County, receiving urban sewage effluent and animal waste from a large number of pig farms. In the

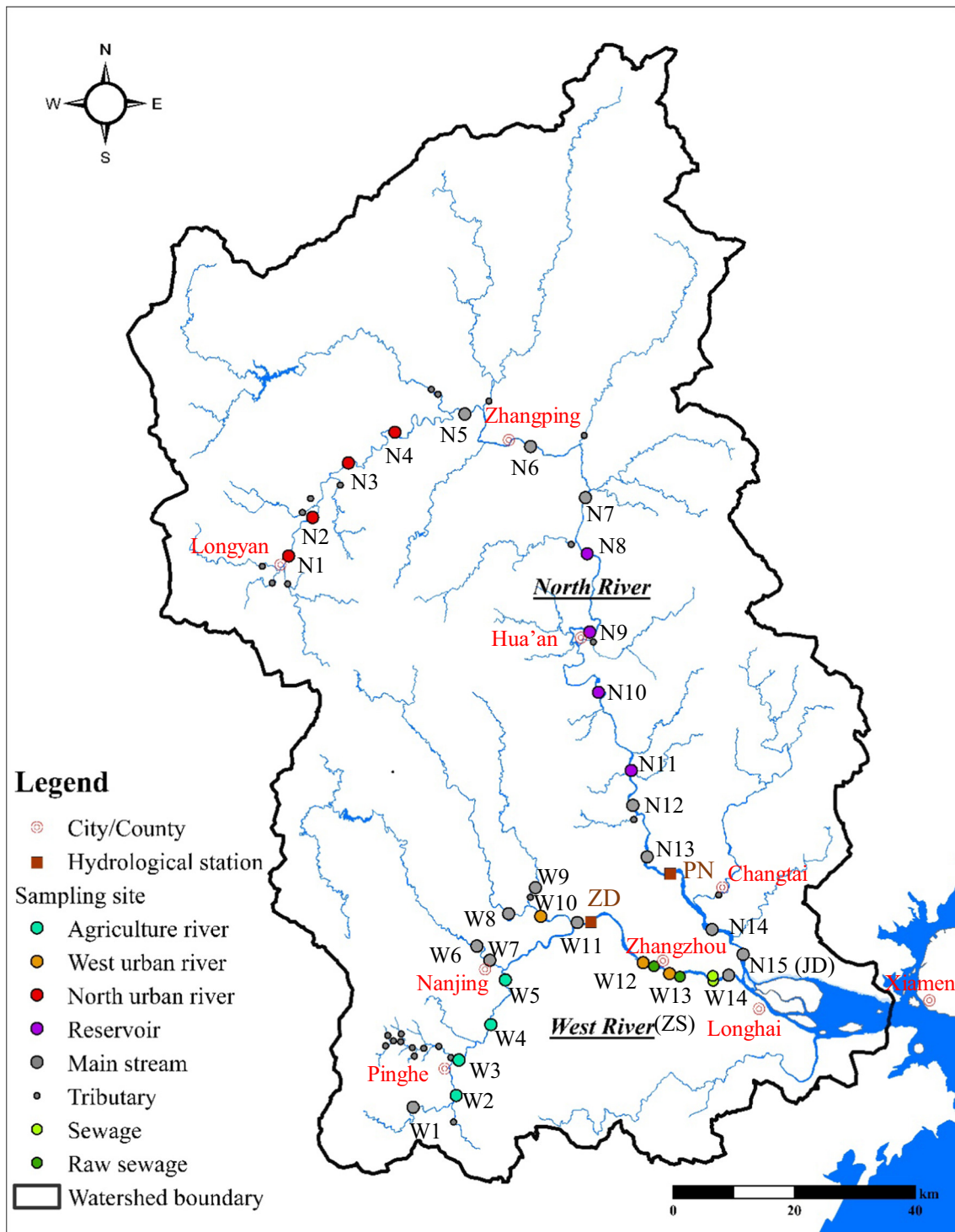


Fig. 1. Map of the Jiulong River Watershed showing the sampling sites. W and N indicates sampling sites in the main stream of the West River and the North River. River sections (Agriculture, West Urban river, North Urban river, Reservoirs) marked by color dots were sampled in wet (July) and dry (November) season of 2018. Additional tributary sites and sewage effluent sites were sampled in dry season (baseflow condition) to track the potential source of P to main stream. High resolution storm observation was conducted at stations N15 (JD) and W13 (ZS) in June 11–13, 2019.

middle section, a number of hydroelectric dams have been constructed in the river channel, forming cascade reservoirs whose function in part is to regulate river flow and sediments, thereby reducing water velocity and suspended particles (Lu et al., 2018). The lower NJR is wider, receiving tributaries which flow through populated towns. The NJR ends at the Jiangdong Reservoir (JD), an important drinking water source for the Zhangzhou and Xiamen urban areas.

2.2. Meteorological and hydrological condition during study period

Two samplings along the river networks were performed in July (wet season) and November (dry season) of 2018. The average temperature and Antecedent Precipitation Index (API), which is the weighted cumulative amount of daily rainfall in the 14 days before the sampling time in July was higher than in November (29.4 °C, 24.2 mm and

22.4 °C, 11.5 mm respectively), as shown in Table 1. Daily NJR mean discharge in July ($108 \text{ m}^3 \text{ s}^{-1}$) was higher than in November ($62.4 \text{ m}^3 \text{ s}^{-1}$) while the WJR discharge was higher in the dry season ($53.1 \text{ m}^3 \text{ s}^{-1}$) compared to the wet season ($35.6 \text{ m}^3 \text{ s}^{-1}$). By contrast, the monthly mean discharges in both rivers were rather similar in the wet and dry seasons (Table 1). A storm event was sampled from June 11 to 13, 2019, at exits from the NJR (JD/N15) and WJR (ZS/W13) (Fig. 1). The daily rainfall during the storm was recorded as 29.3 mm, 16.0 mm and 19.6 mm in the nearest meteorological station in Zhangzhou. Peak discharge during the storm was $2052 \text{ m}^3 \text{ s}^{-1}$ in the NJR and $516.9 \text{ m}^3 \text{ s}^{-1}$ in the WJR.

2.3. Sampling and lab analysis

A total of 29 stations were sampled, with 15 stations in the NJR and 14 stations in the WJR (Fig. 1). Of these stations, seven were characterized as Urban source sites (North Urban: N1–N4; West Urban: W10, W12–W13), four as Agriculture source sites (Agriculture; W2–W5) and four as Reservoir sites (N8–N11) (Fig. 1). The justification and characterization of sites as Urban, Agriculture and Reservoir is explained in detail in Section 4.1. Briefly, Urban represents sites in which the dominant source of P pollution was from domestic sewage, Agriculture sites are where the dominant source of P pollution was from non-point source fertilizers applied to fields and/or orchards, and Reservoir sites are stations sampled in the reservoirs which exist in the main channel of the North River. Additional tributary sites and sewage outlet points were sampled in the dry season (baseflow condition) to provide additional information to characterize the nature of the sources of P pollution to the main river. Surface (0.5 m) water was collected by a 5 L plexiglass sampler for analysis of nutrient forms. Water samples were measured in-situ for physio-chemical indicators, including dissolved oxygen (DO), pH and water temperature using a portable multi-parameter water quality tester (WTW, Germany).

Storm runoff was collected from June 11 to 13, 2019 at the mouth of the NJR (site JD) and WJR (site ZS) continuously (one sample every 1–3 h) using an auto-sampler (GEM+ SMA-S, China). Several samples at the mouth of NJR were unfortunately not collected from 11th 15:00 to 12th 11:00 during the rising hydrograph and maximum flow due to instrument malfunction.

Water samples were divided in two and then filtered through GF/F filters ($0.7 \mu\text{m}$). The filtrate was stored at $4 \text{ }^\circ\text{C}$ and the filters stored frozen at $-20 \text{ }^\circ\text{C}$ before analysis. One of the filters was oven-dried at $105 \text{ }^\circ\text{C}$ to constant weight to determine suspended particulate matter (SPM). The oven-dried filters were combusted at $550 \text{ }^\circ\text{C}$ for 1.5 h and extracted with 1 mol L^{-1} HCl to determine TPP as phosphate. Another filter was extracted into 15 mL Milli-Q water and a subsample (5 mL) taken to measure AP. 5 mL of 3 M HCl (Guarantee Reagent) was then added to a final concentration of 1 M HCl and a subsample taken to measure the PIP. The filtrate was analyzed for dissolved nutrients. DTP was transformed to phosphate with 4% alkaline potassium persulfate. All pretreated phosphate samples and DIP were analyzed as soluble reactive phosphate (molybdate blue reaction) by segmented flow

Table 1
Summary of Antecedent Precipitation Index (API), daily and monthly river discharge for the two sampling periods (July and November 2018).
Adapted from Perrone and Madramootoo (1998).

River	Sampling date	API (mm)	Daily mean discharge ($\text{m}^3 \text{ s}^{-1}$)	Monthly mean discharge ($\text{m}^3 \text{ s}^{-1}$)
North River	20 July	26.9	104.8	151.0
	10 November	8.3	62.4	143.9
West River	20 July	21.4	35.6	45.7
	8 November	14.6	53.1	47.5

Note: Antecedent Precipitation Index (API) = $\sum k^i P_i$, where P_i are precipitation 1, 2, ..., i ($i = 14$) days prior to the event and k is a constant ($k = 0.85$). Three soil antecedent moisture conditions were classified according to API value. Condition I (dry): $0 \leq \text{API} \leq 15 \text{ mm}$; Condition II (average): $15 \leq \text{API} \leq 30 \text{ mm}$; Condition III (wet): $\text{API} > 30 \text{ mm}$.

automated colorimetry (San++ analyzer, Germany). Ammonium ($\text{NH}_4\text{-N}$) and nitrate ($\text{NO}_3\text{-N} + \text{NO}_2\text{-N}$) were analyzed by the same instrument. Dissolved inorganic nitrogen (DIN) was the sum of ammonium and nitrate (see the parallel study by Lin et al. (2020)). DOP was the difference between DTP and DIP, while POP was the difference between TPP and the sum of AP and PIP. The precision for measurements was determined by repeated determinations of 10% of the samples and the relative error was 3–5%. For quality control in the laboratory, a standard reference material provided by the National Environmental Protection Agency was used to check instrument performance, within -1% to $+4\%$ deviations from the standard concentrations.

2.4. Data analysis

The partition coefficient of P (K_d) was calculated by Eq. (1).

$$K_d = [\text{AP}]/[\text{SPM}] \quad (1)$$

where, [AP] was the concentration of phosphate desorbed from the particles by adding MQ water ($\mu\text{g P L}^{-1}$) and [SPM] was the original concentration of particulate matter in the river water (mg L^{-1}).

In addition, we calculated the fraction of inorganic DIP that was adsorbed onto particles by Eq. (2).

$$\text{Adsorbed fraction (\%)} = [\text{AP}] \times 100 / ([\text{AP}] + [\text{DIP}]) \quad (2)$$

where, [AP] was the concentration phosphate desorbed from the particles by adding MQ water ($\mu\text{g P L}^{-1}$) and DIP was the original concentration of phosphate in the river water ($\mu\text{g P L}^{-1}$).

The daily fluxes of P to the head of the estuary were calculated using the concentrations measured at the exits of NJR and WJR (JD/N15 and ZS/W13) and associated river discharge (Eq. (3)).

$$F_i = C_i \times Q_i \times 24 \times 3600 \times 10^{-3} \quad (3)$$

where, F_i is the flux of P during the observation period (kg day^{-1}), C_i is the concentration of P ($\mu\text{g P L}^{-1}$), and Q_i is the daily mean river discharge on the sampling date ($\text{m}^3 \text{ s}^{-1}$). River discharge during the sampling periods was obtained from two hydrological stations (Punan Station (PN) in NJR and Zhengdian Station (ZD) in WJR) (Fig. 1), which were extrapolated to the sampling sites using the ratios of the drainage area between sampling sites and hydrological stations.

To determine P fluxes during the storm event on June 11–13, 2019, hourly discharge was multiplied by the corresponding concentration for each time point. Total P flux (kg P day^{-1}) was estimated as daily mean P load (kg P) normalized by the duration of the storm.

3. Results

3.1. Spatial and seasonal variation of P species among river sections

During the sampling periods, water temperature in the wet season ($29.0\text{--}32.6 \text{ }^\circ\text{C}$) was higher than in the dry season ($23.6\text{--}25.5 \text{ }^\circ\text{C}$) (Table 2). In general, dissolved oxygen (DO) was oversaturated in the wet season except for the average North Urban sites which were slightly undersaturated. During the dry season, the average DO content was somewhat lower with only the West Urban oversaturated. The reservoir stations were saturated and the Agriculture and North Urban were undersaturated. The pH ranged from 6.8 to 8.7 with lower values occurring in the Agriculture river section, especially in the dry season.

Overall the concentrations of TPP and DTP in the NJR decreased from maximum values of $\sim 75 \mu\text{g P L}^{-1}$ TPP and $125\text{--}150 \mu\text{g P L}^{-1}$ DTP in the upper reaches to a minimum value in the middle reaches (N10–N12 for TPP and N8–N9 for DTP) (Fig. 2), and then a slight increase downstream towards the mouth of the river. The concentration of TPP in the WJR fluctuated more widely than in the NJR and generally increased from upstream to downstream. The concentration of DTP along the WJR

Table 2
Summary of physiochemical and mean phosphorus concentrations by river section in wet (July) and dry (November) seasons.

Season	River section	Water temperature (°C)	pH	DO (%)	TP ($\mu\text{g P L}^{-1}$)	DTP	DIP	DOP	TPP	AP	PIP	POP	SPM (mg L^{-1})
Wet season (July 2018)	Agriculture	32.3 ± 1.0	7.5 ± 0.8	123.2 ± 35.8	159.0 ± 34.7	117.3 ± 55.5	76.4 ± 42.7	40.8 ± 14.5	41.7 ± 22.9	5.5 ± 4.7	12.9 ± 2.2	23.3 ± 16.3	9.4 ± 4.1
	North Urban	29.0 ± 1.0	7.4 ± 0.1	84.9 ± 12.0	182.8 ± 30.4	117.5 ± 23.3	86.0 ± 21.6	31.5 ± 3.8	65.4 ± 7.6	5.4 ± 0.0	31.3 ± 7.4	28.7 ± 7.5	21.4 ± 1.6
	West Urban	32.6 ± 0.3	8.1 ± 0.4	149.2 ± 12.1	102.0 ± 12.0	39.8 ± 4.0	11.5 ± 4.6	28.3 ± 1.1	62.2 ± 10.0	2.7 ± 1.8	10.3 ± 4.2	49.2 ± 7.7	15.0 ± 3.5
Dry season (November 2018)	Agriculture	24.4 ± 0.6	6.8 ± 0.1	91.5 ± 11.9	114.7 ± 13.1	81.3 ± 9.4	78.1 ± 7.9	3.2 ± 2.0	33.4 ± 11.5	8.9 ± 2.7	12.7 ± 3.8	11.8 ± 5.4	12.9 ± 0.2
	North Urban	23.6 ± 0.7	7.4 ± 0.2	78.9 ± 9.5	138.7 ± 39.1	83.4 ± 36.3	66.5 ± 27.2	17.0 ± 11.6	55.2 ± 17.1	11.4 ± 4.6	35.1 ± 15.5	8.7 ± 14.5	7.3 ± 4.7
	West Urban	25.5 ± 1.3	7.7 ± 0.6	127.5 ± 33.4	115.2 ± 35.8	44.5 ± 23.6	30.2 ± 12.4	14.3 ± 11.9	70.7 ± 13.8	19.7 ± 5.6	8.9 ± 0.6	42.1 ± 15.3	10.6 ± 2.0

Note: data shown as mean ± one standard deviation for Agriculture (W2–W5), North Urban (N1–N4) and West Urban (W10, W12–W13).

remained roughly constant with slightly higher concentrations during the wet season than in the dry season (Fig. 2).

3.2. Characterization of the P speciation of the major pollution sources to the river channel and seasonal changes

In order to characterize the P speciation of the most important pollution sources to the river channel, three river sections were identified as having a single dominant source of nutrient pollution (Fig. 1). These were the headwaters of the West River (Agriculture source), the headwaters of the North River (North Urban source) and the lower West River channel as it passed through Zhangzhou (West Urban source). The data presented in Table 2 shows the average concentration of measured P species for these stations during both the wet and dry season sampling. We chose to use the dry season (baseflow condition) values to characterize the individual pollution sources. The TP of the Agriculture source was $114.7 \pm 13.1 \mu\text{g P L}^{-1}$ of which $33.4 \pm 11.5 \mu\text{g P L}^{-1}$ was as TPP and $81.3 \pm 9.4 \mu\text{g P L}^{-1}$ was as DTP. The POP/TPP and PIP/TPP fractions were rather similar at ~40% while almost all of the DTP was as DIP (Fig. 3). The West Urban source had similar TP to the Agriculture source ($115.2 \pm 35.8 \mu\text{g P L}^{-1}$) but different speciation with much higher TPP ($70.7 \pm 11.5 \mu\text{g P L}^{-1}$) most of which was POP (Fig. 3). The DTP was almost entirely DIP. The North Urban source in the dry season had somewhat higher TP, and intermediate TPP compared with the West Urban source (Table 2). Most of the TPP was PIP with a rather low amount of POP. Approximately 60% of the DRP was DIP with the rest as DOP (Fig. 3). The AP/TPP fraction was higher in all sources during the dry season than during the wet season.

Kd is a measure of the ability of SPM to reversibly adsorb phosphate onto the surface of particles. In the Jiulong River there were major increases in Kd in the Urban sources between the dry season and the wet season while Kd remained relatively constant in the Agriculture source (Table 3). Similarly, there was a higher proportion of DIP adsorbed onto particles during the dry season compared with the wet season. In general, the TP concentration was also higher during the wet season than the dry season while the TPP was of a similar range to that in the dry season.

In order to estimate the effect of impoundment in cascade reservoirs in the main channel of NJR, we compared the P speciation in the river upstream and downstream of the reservoirs with samples collected within the cascade reservoirs (Table 4). In both the wet and dry seasons, the DTP was considerably reduced in the reservoirs compared to samples taken in the river adjacent to the reservoirs ($27.1\text{--}34.5 \mu\text{g P L}^{-1}$ compared with $34.9\text{--}68.6 \mu\text{g P L}^{-1}$). During the dry season most of the DRP was as DIP in the reaches adjacent to the reservoirs but the fraction was reduced within the reservoirs (Fig. 4). At the same time, the relative amount of POP as a fraction of TPP increased in the reservoirs compared to the waters arriving from upstream (Table 4, Fig. 4). The proportion of AP/TPP remained relatively constant through the reservoir sites during the dry season. There were similar patterns in the wet season with most of the DRP reaching the reservoirs as DIP, which was reduced in the reservoir, while there was a higher proportion of POP in the reservoirs compared to the in-coming water. The AP concentration, Kd and fraction attached to particles were lower for almost all samples during the wet season compared with the dry season (Table 3).

3.3. Temporal variation of P species at river mouths during a storm event in 2019

Concentrations of SPM and P species changed with river discharge in the WJR during the storm event (Fig. 5). For the WJR, SPM (mg L^{-1}) doubled at the beginning of the rising hydrograph and then dropped for the remaining rising hydrograph. There was then a dramatic increase at the beginning of the falling hydrograph, which remained

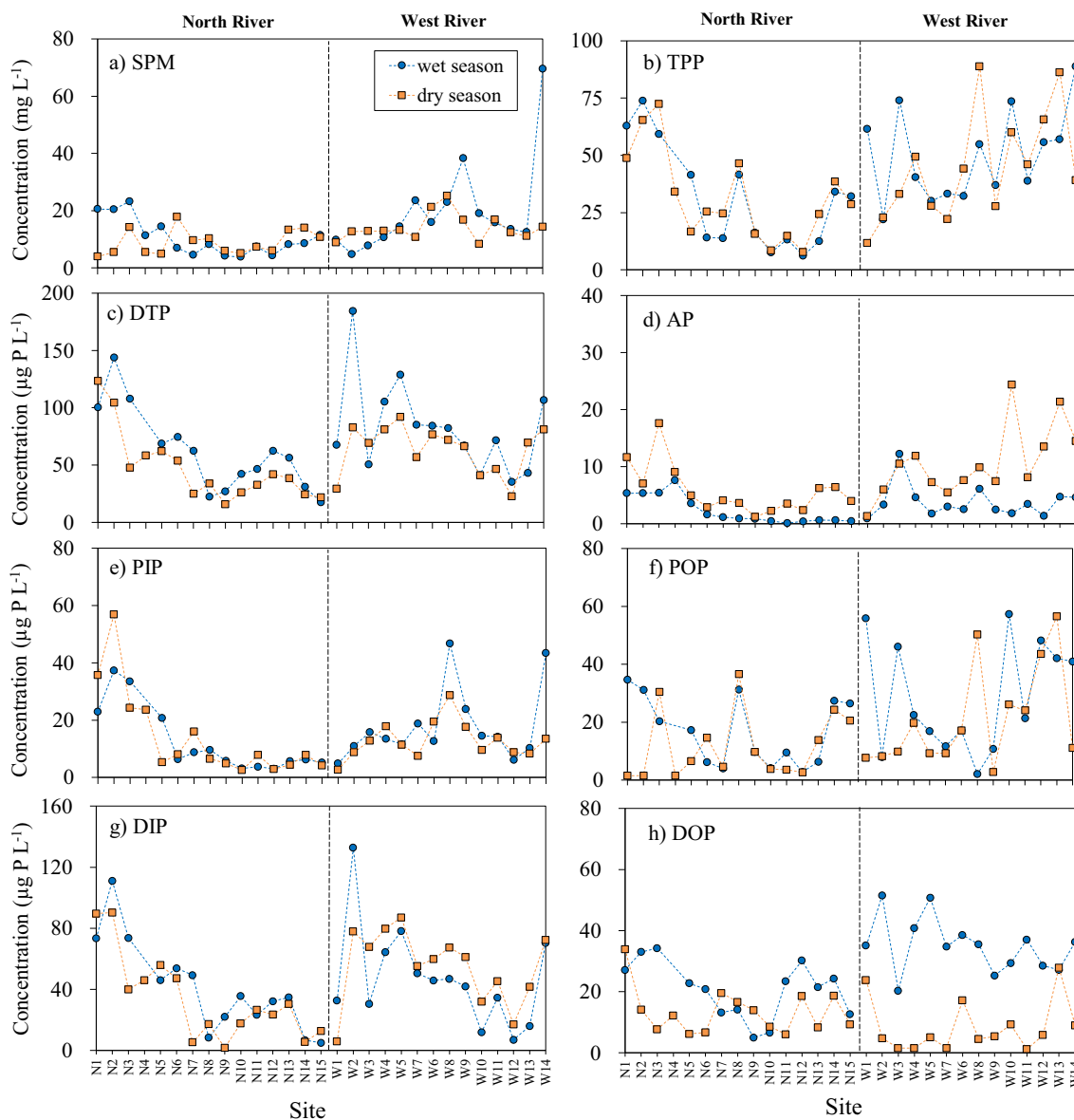


Fig. 2. Changes of concentrations of SPM and phosphorus speciation along the North and West Jiulong River in the wet (July) and dry (November) seasons in 2018.

constant though somewhat scattered at 3 times the initial value. TPP followed SPM closely with an increase at the beginning of the storm, a decrease for the remainder of the rising hydrograph followed by a rapid increase during the falling hydrograph. As with SPM and TPP there was an increase in PIP and POP at the beginning of the hydrograph, a decrease during the main section of the increasing hydrograph and then an increase at the maximum and during the falling hydrograph. In contrast to TPP and SPM, the values for POP and PIP fluctuated somewhat during the falling hydrograph. DIP and DOP were different from the other P species. During the storm DIP increased rapidly at the beginning of the rising hydrograph, and then dropped back almost to pre-storm concentrations at the maximum storm flow. However, this decrease was later in the storm than the decrease in TPP. Having reached a minimum value at the peak of the hydrograph, it then increased again at the beginning of the falling hydrograph to a new steady state for the rest of the falling hydrograph. DOP also behaved differently from all other P species in that its concentration remained relatively constant throughout the entire storm. AP was a minor component of TP. The AP pattern broadly followed changes in TPP (and not DIP) in that it dropped as TPP and PIP dropped during the rising hydrograph from around $9.3 \mu\text{g P L}^{-1}$ and then increased at

the maximum flow, before remaining constant at a new steady state value of $8.2 \mu\text{g P L}^{-1}$ during the falling hydrograph. For the whole storm event in WJR, DTP dominated in TP (70%) while TPP had a relatively small fraction (30%) compared with NJR (52% DTP and 48% TPP).

The pattern of the storm in the NJR was more difficult to follow because the sampler failed during the increasing hydrograph and the maximum flow period, which were the regions of maximum change in the WJR (that is, the pattern for the rising hydrograph and maximum flow were lost) (Fig. 6). In general, the pattern was similar to that observed in the WJR. In particular the SPM on the falling hydrograph was higher than for the baseflow before the storm (and approximately twice as high as WJR). TPP increased at the beginning of the rising hydrograph and reached a steady state value on the falling hydrograph which was higher than baseflow. PIP and POP also started to increase at the beginning of the rising hydrograph and reached a new higher value on the falling hydrograph. In contrast to the WJR, the values for PIP and POP in the NJR were stable on the falling hydrograph. DIP also started to increase on the rising hydrograph and reached a new stable higher value on the falling hydrograph. The pattern for AP was also similar to that for the WJR.

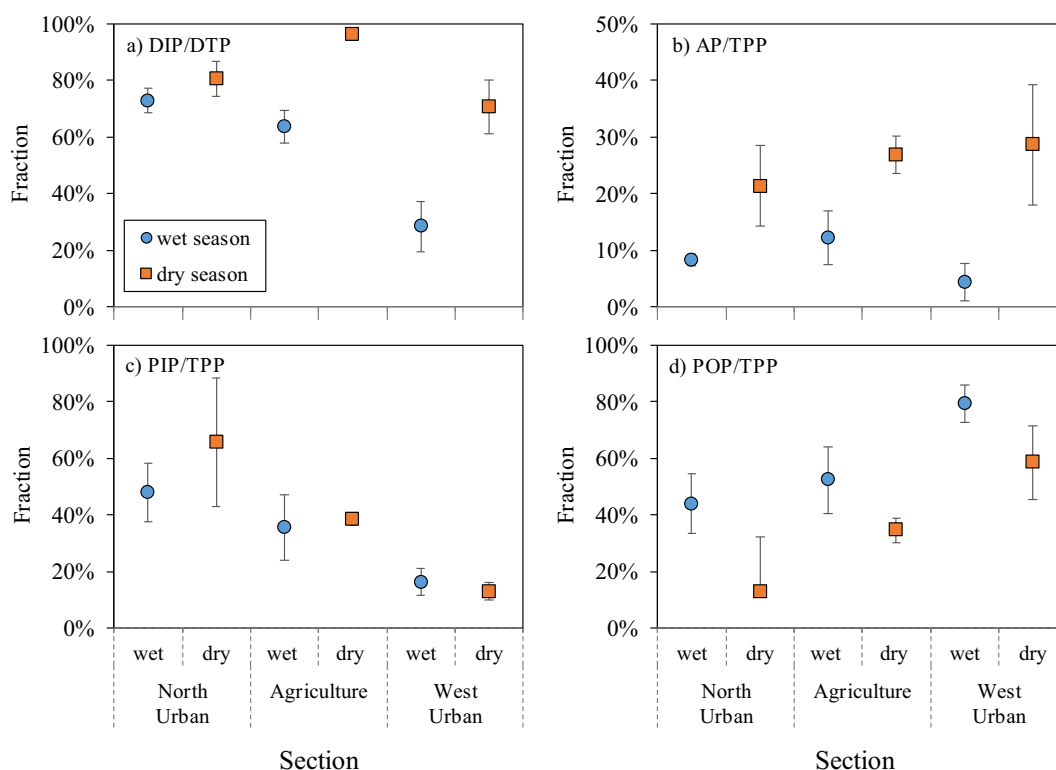


Fig. 3. Phosphorus fractions measured in different river sections which are dominated by particular types of source activities.

3.4. The concentration and flux of baseflow and stormflow P speciation to the head of estuary

The concentrations and fluxes of P species at river mouths (stations ZS and JD) during the wet and dry seasons were taken to be average baseflow values flowing from the catchment to the head of the estuary (Table 5 and Fig. 7). The dominant form of P leaving the watershed was as TPP, representing 55–57% of the TP from the WJR and 57–65% leaving the NJR. As noted above, the water flow during wet and dry seasons are relatively similar due to the regulation of dam reservoirs in the river, and thus the differences in fluxes are dominated by changing concentrations. Storm flow is much higher than normal river flow, and as a result P flux was greater in the NJR than in the WJR, and event mean concentration (EMC) of P species were larger in the stormflow period compared to the background (baseflow) period.

3.5. N:P ratios under baseflow and storm flow conditions

The molar ratios of DIN to DIP differed between river sections and between seasonal sampling and storm observation (Fig. 9). In general, the N:P ratio in the WJR was higher than in the NJR. Agriculture and

West Urban sources had the largest N:P ratios (relatively high DIN) among all river sections. For the NJR, the N:P ratio was elevated from the upstream to reservoirs (relatively low DIP) and decreased in the downstream. Higher N:P ratios were found in the dry season than in the wet season for the Agriculture, West Urban and North Urban rivers, while a higher ratio occurred in the wet season for the reservoirs. In addition, a higher N:P ratio in storm runoff at exits of the WJR (W13) and the NJR (N15) was observed in the rising hydrograph than in the falling hydrograph of storm flow.

4. Discussion

4.1. Characteristics and source tracking of river P

The sources of nutrient pollution in the Jiulong River system are complex, as they are in many such densely populated catchments. The sources include agricultural, industrial and domestic waste inputs and both point and non-point sources (Yu et al., 2015). In a parallel study of N pollution in the Jiulong River watershed (Lin et al., 2020), the sources of pollution were simplified into two major types. The first was agricultural runoff, which was non-point source pollution in which the

Table 3
K_d values and adsorbed fraction by river section in the wet (July) and dry (November) seasons of 2018.

Period	Agriculture	North Urban	West Urban	Reservoir
	K _d (μg mg ⁻¹)			
Wet season (July 2018)	0.70 ± 0.62	0.35 ± 0.21	0.19 ± 0.15	0.09 ± 0.07
Dry season (November 2018)	0.69 ± 0.21	1.78 ± 0.80	1.96 ± 0.90	0.37 ± 0.10
Period	Agriculture	North Urban	West Urban	Reservoir
	Adsorbed fraction (%)			
Wet season (July 2018)	26.5 ± 12.6	12.5 ± 5.9	20.5 ± 10.2	9.1 ± 4.4
Dry season (November 2018)	41.1 ± 2.7	26.3 ± 12.7	68.2 ± 6.4	36.6 ± 11.9

Note: data shown as mean ± one standard deviation for Agriculture (W2–W5), North Urban (N1–N4), West Urban (W10, W12–W13) and Reservoir (N8–N11, N15).

Table 4
Comparison of the concentrations of mean phosphorus species between the reservoir and upstream and downstream sites in the North River.

Season	River section	TP	DTP	DIP	DOP	TPP	AP	PIP	POP	SPM (mg L ⁻¹)
		(µg P L ⁻¹)								
Wet season (July 2018)	Upstream	91.8 ± 17.1	68.6 ± 6.0	49.7 ± 3.9	18.9 ± 5.0	23.2 ± 15.8	2.1 ± 1.2	11.9 ± 7.7	9.1 ± 7.0	8.7 ± 5.2
	Reservoirs	54.2 ± 9.5	34.5 ± 11.6	22.2 ± 11.1	12.3 ± 8.4	19.7 ± 15.0	0.6 ± 0.3	5.5 ± 2.9	13.6 ± 12.0	5.9 ± 2.2
	Downstream	67.5 ± 2.0	49.9 ± 16.6	24.5 ± 15.5	25.3 ± 4.4	17.6 ± 14.6	0.6 ± 0.1	5 ± 1.7	12.1 ± 13.2	7.0 ± 2.3
Dry season (November 2018)	Upstream	69.2 ± 17.0	46.9 ± 19.6	36.1 ± 27.1	10.8 ± 7.6	22.3 ± 4.8	4.0 ± 1.0	9.8 ± 5.5	8.6 ± 5.3	10.8 ± 6.5
	Reservoirs	48.6 ± 22.4	27.1 ± 8.3	15.8 ± 10.3	11.3 ± 4.8	21.5 ± 17.0	2.6 ± 1.1	5.4 ± 2.2	13.4 ± 15.6	7.2 ± 2.2
	Downstream	58.5 ± 7.5	34.9 ± 9.4	19.8 ± 12.7	15.2 ± 5.9	23.6 ± 15.3	5.0 ± 2.2	5.1 ± 2.5	13.6 ± 10.8	11.1 ± 4.4

Note: data shown as mean ± one standard deviation for upstream (N5–N7), reservoirs (N8–N11) and downstream (N12–N14).

major source was excess fertilizers applied to fields and orchards and subsequently discharged into the upper West River. This was characterized by a NO₃-N/DIN fraction close to 100%. This high ratio was due both to nitrate in the originally applied fertilizer and to nitrification in the fields converting NH₄-N in the fertilizer to NO₃-N. The second major source of external pollution to the Jiulong River was domestic sewage effluent discharged either directly or indirectly from secondary sewage treatment works. The characteristic of sewage effluent is that there is a relatively higher fraction NH₄-N of DIN in the discharge as it reaches the river. This category of waste could also include waste from domestic sewage in towns and villages as well as major cities and might also include waste from intensive pig farms.

In this study, a similar division of pollution sources was developed by identifying sub-catchments which have a single dominant pollution source. This division was used to develop characteristics of the P speciation of these two major pollution sources into the Jiulong River. The headwaters of the West River are dominated Pomela orchards; according to our survey, these orchards receive intensive applications of chemical fertilizers including phosphate (~100 kg P ha⁻¹) mainly in May–July (wet season) and January (dry season). Here we sampled the upper tributary (W2–W5) in November 2018 to characterize the P pollution being supplied by agricultural pollution to the West River. The TP of this source was 114.7 ± 13.1 µg P L⁻¹, TPP was 33.4 µg P L⁻¹ with an SPM of 12.9 ± 0.2 mg L⁻¹ (Table 2). In the same stations, Lin et al. (2020) reported that

the proportion of nitrate (NO₃-N) to dissolved inorganic nitrogen (DIN) was greater than 99%, which is characteristic of non-animal agricultural pollution. For these stations the DIP/DTP fraction was 96% and the POP/TPP fraction was 30% (Table 2, Fig. 3). This pattern seems reasonable for a P pollution source that was mainly excess potentially soluble inorganic fertilizer being flushed off the fields into the river channels. The relatively low amount of organic P could be due to plant debris in the river channels and/or remnant organic P from the manure added to the field in January. However, it should be noted that none of the river P in this study, even from an agricultural area which is almost entirely Pomela orchards, are totally from one source, and there could also be some domestic sewage from the small farming communities in the catchment. An important additional factor in the flushing of P pollution into the river channels is the amount of SPM, which is generally related to soil erosion (Zuijdggest and Wehrli, 2017). For those agricultural stations when the TPP: SPM ratio ≥ 2.0 µg mg⁻¹, the POP/TPP fraction range was 6%–30%, while when the TPP: SPM ratio < 2.0 µg mg⁻¹, the mean POP/TPP fraction was 37%. This implies that when there was more soil erosion (higher SPM) there was also relatively more organic P eroded into the river channels. The fraction of DIP adsorbed onto particles was relatively constant between the wet and dry seasons, and Kd was intermediate between the values from the Urban sources in the dry and wet seasons (Table 3).

In contrast to agricultural pollution, domestic sewage has a relatively high proportion of NH₄-N (Lin et al., 2020). Here we selected the sites in

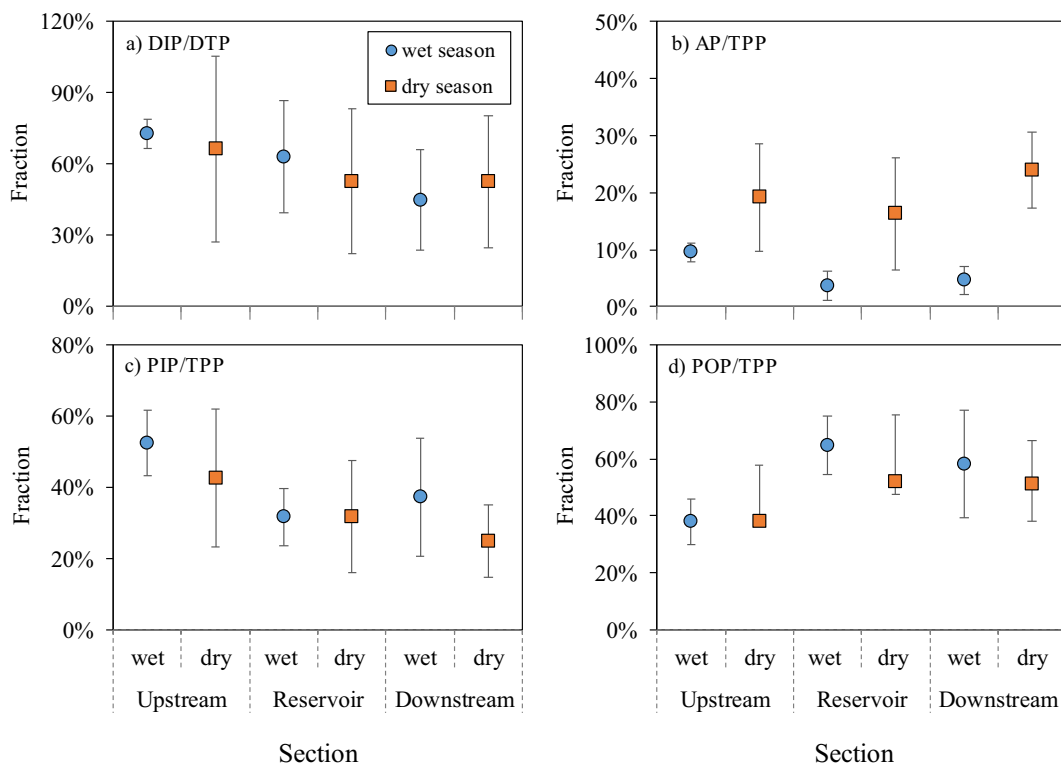


Fig. 4. Phosphorus fractions measured for average reservoir (N8–N11) compared with the upstream (N5–N7) and downstream (N12–N14) sites.

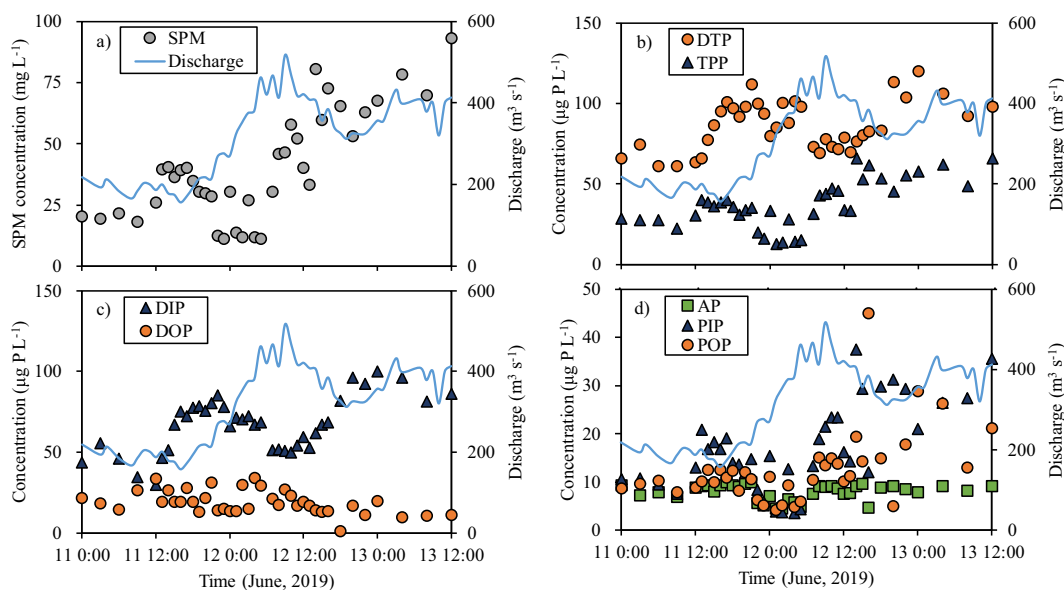


Fig. 5. Evolution of river discharge, SPM and P species during the observation of storm event at ZS station of West Jiulong River in June 11–13, 2019.

which $\text{NH}_4\text{-N}$ was relatively higher and there was the presence of point source discharges from domestic sewage works. We chose two type areas, one of which in the lower West River catchment was located close to the outlet of the wastewater treatment plants from Zhangzhou ($n = 3$) (stations W10, W12 and W13). At these stations the $\text{NH}_4\text{-N}/\text{DIN}$ fraction was $5.6 \pm 2.8\%$, the TP and SPM was rather similar to the Agriculture source (Stations W2–W5), $115.2 \pm 35.8 \mu\text{g P L}^{-1}$ and $10.6 \pm 2.0 \text{ mg L}^{-1}$. However, the P speciation was very different. The TPP was more than double at $70.7 \pm 13.8 \mu\text{g P L}^{-1}$, with the organic P phases much higher, POP was $42.1 \pm 15.3 \mu\text{g P L}^{-1}$ and DOP was $14.3 \pm 11.9 \mu\text{g P L}^{-1}$, which were 3.5 and 4.5 times higher than in the Agriculture source. Sewage effluent contains a high fraction of organic matter even after secondary treatment and this is the source of the higher fraction of organic P into the river channel. It was observed that much of the SPM was organic particles ($>3.5 \text{ mg P of POP per gram of SPM}$) in Urban sites (W12, W13) in contrast to the Agriculture source ($<1.0 \text{ mg P of POP per gram of SPM}$).

The North Urban source was not collected adjacent to single major sewage effluent discharges as was the case for the West River. Stations N1–N4, which were used to define the North Urban source, were collected in the main river channel as it passed through Longyan, an area with high population density and intensive pig farming. It was defined as North Urban based mainly on the fraction of $\text{NH}_4\text{-N}$, which was greater than 20% (Lin et al., 2020). The TP and SPM of this source was rather higher than the West Urban source ($138.7 \pm 39.1 \mu\text{g P L}^{-1}$) while the SPM was slightly lower at $7.3 \pm 4.7 \text{ mg L}^{-1}$ (Table 2). As with the West Urban, the TPP was much higher than the Agriculture source at 55.2 ± 17.1 , as was the DOP at $17.0 \pm 11.6 \mu\text{g P L}^{-1}$. Somewhat surprisingly, the POP was rather low at $8.7 \pm 14.5 \mu\text{g P L}^{-1}$ (Table 2), possibly because this source was more diffuse (non-point source) compared with the West Urban source and so although the ammonium remained high, some of the POP had been converted into DIP by microbial action and other decay.

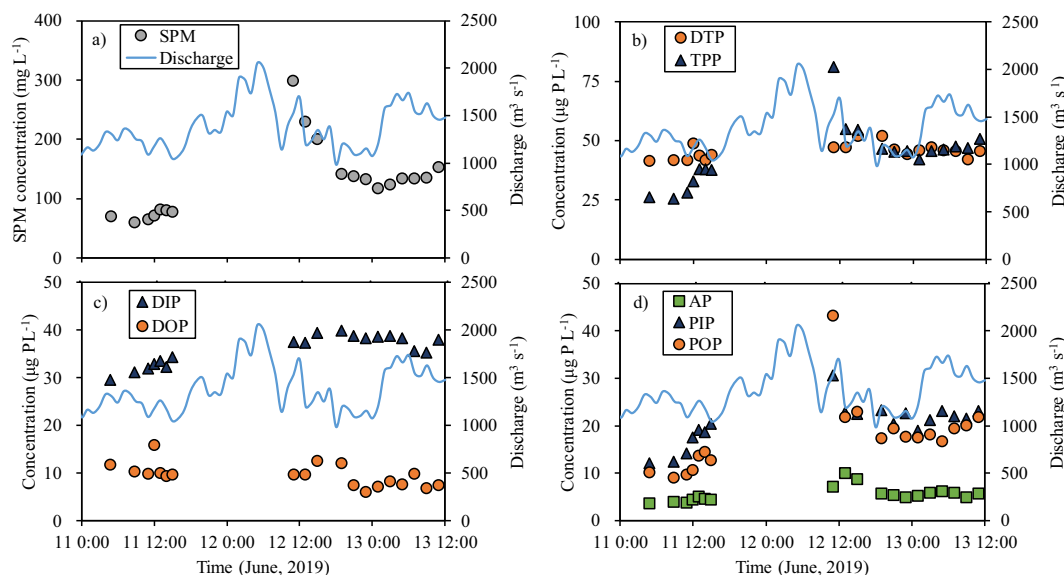


Fig. 6. Evolution of river discharge, SPM and P species during the observation of storm event at JD station of North Jiulong River during June 11–13, 2019. Measurement was not fully conducted in the rising flow period due to auto-sampler malfunction.

Table 5
Concentration and flux of P species during seasonal sampling at the exits from the North River and West River to head of estuary.

Period	Station	TP	DTP	DIP	DOP	TPP	AP	PIP	POP
		Concentration ($\mu\text{g P L}^{-1}$)							
Wet season (July 2018)	N15	49.7	17.5	4.9	12.6	32.2	0.5	5.2	26.5
	W13	100.1	43.0	15.9	27.1	57.1	4.7	10.5	42.1
Dry season (November 2018)	N15	50.5	21.9	12.6	9.3	28.6	4.0	4.1	20.5
	W13	155.8	69.6	41.7	27.9	86.2	21.4	8.3	56.5
Period	Station	TP	DTP	DIP	DOP	TPP	AP	PIP	POP
		Flux (kg P day^{-1})							
Wet season (July 2018)	N15	475.3	167.4	46.9	120.6	307.9	4.6	50.2	253.2
	W13	324.1	139.4	51.5	87.8	184.7	15.3	33.3	136.2
Dry season (November 2018)	N15	311.8	135.1	77.8	57.4	176.7	24.7	25.4	126.7
	W13	754	336.7	201.8	135.0	417.3	103.4	40.4	273.6

When comparing the agricultural and urban sources during the wet warm season (July) with the dry (November) season, it was found that there was comparatively little difference for the West Urban source (Table 2), which was the most homogeneous source (domestic sewage effluent from point sources). While the effluent had slightly less TP ($102 \pm 12.0 \mu\text{g P L}^{-1}$) compared with the dry season ($115.2 \pm 35.8 \mu\text{g P L}^{-1}$), other parameters such as TPP, PIP, POP, and DTP were quite similar (<15% deviation). In contrast, the Agriculture and North Urban source were considerably different during the wet warm season. In particular, in both sources there was a higher fraction of organic P species in the wet season. Thus, for the Agriculture source the TP was 38% higher (with most of the difference being POP) which was more than double the TP in the dry season, while DOP was more than 12 times higher. Since this difference could not be due to changes in chemical P fertilizer added, it was concluded that this was due to organic P being eroded from the fields (manure is added to the fields in January) or washed out of drainage channels and/or village sewage systems as the amount of rainfall increased. Similarly, there was more total P (30% higher) in the North Urban source in the wet season than in the dry season. This was also mainly due to an increase in POP (3.3 times higher) and DOP (1.8 times higher) though in the case of North Urban, DIP also increased by ~30%. It is more difficult to assign a cause to these differences since the North Urban is less homogeneous, though for the explanation may be similar to that for the Agriculture source, namely that organic matter is eroded from fields or washed out of drainage channels and sewage systems.

4.2. Hydro-biogeochemical changes in P speciation found in the river channel

There were systematic changes in P speciation in the North River downstream of the four urbanized stations (N1–N4) in the upper

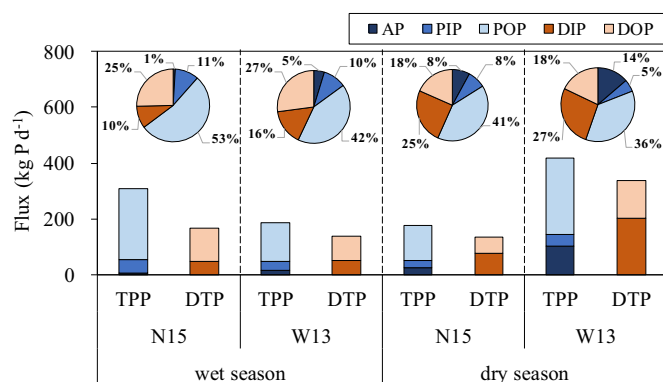


Fig. 7. Particulate and dissolved phosphorus flux (bar) and fraction of P species in TP (pie) at the North River exit (N15/JD) and the West River exit (W13/ZS) of the Jiulong River in wet (July) and dry (November) seasons in 2018.

reaches of the river (Fig. 2). There was a large decrease in TPP, DTP, PIP, and DIP but a smaller decrease in POP and DOP. This spatial pattern was largely due to dilution by tributaries which had lower levels of contamination. The pattern in the West River was more complex mainly because some of the stations were inside tributaries. There were substantial pollution sources downstream of the initial intensive agricultural locations and thus P was added in some places and diluted in others. In addition to these external changes affecting the P chemistry, there are also biogeochemical changes occurring within the river channel itself.

Once P reaches the main river channel, DIP can be removed from the water column by inorganic adsorption processes and by biological uptake. In this study the inorganic uptake processes were estimated by the determination of K_d and the fraction adsorbed. It was found that in the dry season 26%–68% of the DIP was adsorbed onto SPM (Table 3). In aquatic systems it is considered that this adsorbed P remains potentially bioavailable and if DIP is removed by biological uptake processes, it can be replaced by inorganic adsorbed P (Slomp, 2011). This process was seen in the reservoirs (see below). In the wet season, the fraction of phosphate adsorbed onto particles was considerably less than in the dry season (Table 3) even though there was only a small decrease in SPM (Table 2). At the same time, the amount of SPM decreased substantially from the Urban sites (N1–N4) to the downstream. This was due to less P being adsorbed onto the particles, since the DIP in the water column was approximately the same. It is possible to speculate that during the wet season the nature of the particles in the water column may have been different, with a higher PIP:POP ratio. However, since no detailed study of the nature of these particles was made it is not possible to know why there was less P adsorbed.

Phosphate can be biologically uptaken into POP. However, there was no systematic change in POP downstream of the major sources in the North River, while in the West River there were fluctuating values of POP. It is not possible to determine whether biological uptake processes were minor in the Jiulong River (maybe due to light limitation in the turbid water or simply that there were so many complex interactions, including dilution by tributaries, microbial decomposition, sedimentation, etc.). Therefore, no clear pattern of changes in POP in the river channel could be seen. In order to determine the rate of biological uptake within the water column it would be necessary to carry out a series of biological rate experiments which was beyond the scope of this study.

There are a number of dams across the North River channel which cause reservoirs to form behind them (N8–N11). It is characteristic of reservoirs that the water flow is reduced and so SPM is sedimented out. Since the water column is less turbid there is increased phytoplankton growth and thus P uptake (Maavara et al., 2015; Maavara et al., 2020). In this study, we compared the stations immediately upstream (N5–N7) and downstream (N12–N14) of the reservoirs to determine whether the effect of the reservoirs on P chemistry could be seen (Table 4). During the dry season there was a small decrease in SPM in

the reservoirs compared to the adjacent stations ($10.9 \pm 5.0 \text{ mg L}^{-1}$ compared with $7.9 \pm 2.5 \text{ mg L}^{-1}$). There was also a decrease in DIP and AP and an increase in POP, which is likely associated with increased phytoplankton uptake of P in the reservoirs (Lu et al., 2016). TPP remained essentially constant at $23.0 \mu\text{g P L}^{-1}$ in part because the amount adsorbed on particles decreased, likely due to release and biological uptake. During the wet season we observed a similar pattern as SPM decreased from 8.7 to 5.9 mg L^{-1} . There was also a decrease in DIP and AP and an increase in POP while TPP decreased substantially. These changes in P chemistry are consistent with particulate matter being sedimented out and increased biological uptake of P in the reservoirs. This pattern can be seen despite the confounding factors such as small tributaries reaching the river and at least some recycling of P from the sediment within the reservoirs.

4.3. Effect of storms on the cycling and discharge of P down the river system

The pattern of P speciation through the storm in the WJR in June 2019 (Fig. 5) provides information on the nature and location of anthropogenic P mobilized by the increased river flow. At the beginning of the storm there was an increase in SPM with its associated particulate P (TPP, PIP and POP), likely due in part to resuspension of particulate P in the river channel as well as rapid soil erosion from the adjacent fields. There was a tight correlation between TPP and SPM throughout the increased flow of the storm ($\text{TPP} = 0.6561 \times \text{SPM} + 11.26$, $R^2 = 0.95$, $p < 0.01$), which implies a single type of SPM being mobilized during storm flow. During this early phase of the storm DIP also increased, possibly due to remobilization from sediment pore waters. However, it is more likely to be due to phosphate being washed off the fields, especially since the length of the increase in DIP was longer than that of the particulate P phases. Particulate P decreased presumably due to dilution during the rising hydrograph (Fig. 5). It is also noted that DOP did not increase during this early phase of the storm. Pollution from agricultural sources contains a relatively high DIP: DOP ratio, suggesting that the initial effect of the storm was to wash excess fertilizer P from surface agricultural fields. However, rather rapidly the TPP decreased on the rising hydrograph, which implies that the SPM was being diluted by increased water flow. At maximum flow all P species (dissolved and particulate) were somewhat diluted by the increased amount of water being fluxed down the river. However, for all P species there was an increase again in the falling hydrograph with higher concentrations of TPP, POP, PIP, and DIP than were present before the storm (Fig. 5). This is likely due to interflow driven release of stored P from surface soils and other longer-term sources compared to the initial flux from the fields. It is not known how long this increase was sustained after the peak of the storm passed since sampling stopped ~24 h after peak discharge and the system had not returned to baseflow. AP is generally considered to be regulated by a rapid equilibration between DIP and particulate matter. In this storm the AP was a similar steady state early in the storm and during the falling hydrograph, and AP only decreased for a short period during the rising hydrograph when SPM and particulate P decreased and DIP remained higher, suggesting that the storm had mobilized new SPM which had not yet reached equilibrium with DIP. The pattern for NJR was consistent with that observed for WJR (Fig. 6) but due to the missing data during the rising hydrograph and maximum flow it is not possible to confirm this pattern in detail.

Similar to previously reported patterns of nutrient export via storm flow (Bowes et al., 2005; Chen et al., 2012; Chen et al., 2015; House and House and Warwick, 1998), a hysteresis effect was also observed with P concentrations at the discharge point being different on the rising and falling limbs of the hydrograph (Fig. 8). In general, most P species showed an anticlockwise trajectory around the high flow period in WJR, indicating a flushing of P pollutants from the polluted areas close to the sampling station (W13), resulting in a sharp increase at the beginning of the storm and subsequently P species from secondary sources

during the falling hydrograph. This is different from NJR samples in a previous storm where DRP and DOP showed a clockwise trajectory (Chen et al., 2015). The difference implies a dilution of within channel P by increased storm runoff caused by the delay of remote P sources in the upper North River reaching the sampling station at the exit from the NJR.

Storm size impacts the dynamics of river P concentration, composition and flux (Table 6). The P flux of NJR was higher than WJR because of the greater water flow, and the EMC of WJR was greater than the NJR due to the greater baseflow P concentrations in the West River draining an intensively fertilized agricultural orchard area (upper WJR) and highly populated area close to the sampling station in the lower WJR (Table 6). Phosphorus fluxes and EMC were generally lower in the smaller storm (June 2019) than the larger storm (July 2013) (Chen et al., 2015). For NJR in June 2019, greater DIP: DTP (0.78) and lower TPP: TP (0.51) flux ratios were found compared to the larger storm in 2013 (Table 6), suggesting relatively more DIP (more washout with less dilution) and less TPP (less soil erosion) export during the less intensive storm.

The baseflow exiting the West River during normal flow is similar in nature to the West Urban source with higher POP than PIP in the particulate fraction and higher DOP compared with DIP in the wet season, and lower DOP compared with DIP in the dry season (Fig. 7). This pattern is expected since the West Urban source fluxes into the river near its mouth. By the time water from the Agriculture source has reached the mouth of the river it has been transformed by processes within the river channel and by addition and dilution of pollutants in the channel downstream of this important source. The dominant form of P leaving the North River catchment is as organic P (53% POP and 25% DOP for the wet season, Fig. 7). This represents a net transformation of P from the dominantly inorganic P in the North Urban source at the headwaters of the catchment to the waters flowing out of the catchment at N15. An important vector of these changes is biological uptake of P within the river channel, including the reservoir at station N15. However, as with the West River (and indeed also all modern rivers) the actual combination of addition and dilution processes into the channel and internal P cycling is complex and varies with seasons and water flow.

The fluxes out of the catchment are much greater during the storm than under baseflow, with the TPP and DTP being greater than an order of magnitude higher during storm flow from the NJR, which itself is 2–3 times higher than that from the WJR (Table 6). This is characteristic of the Jiulong River, and most other rivers, in that by far the greatest daily flux of nutrients occurs during storm flow (Correll et al., 1999; Mok et al., 2019). Depending on the frequency of storms, this represents a disproportionately high fraction of the total flux of nutrients out of the catchment to the coast (Gao et al., 2018).

The DIN:DIP molar ratio within the Jiulong River system (Fig. 9), and particularly in the river channels identified as Agriculture and West Urban sources, was well in excess of the canonical Redfield ratio of 16:1 and even in excess of the much higher DIN:TDP ratio of 53–250:1 suggested by Maberly et al. (2002) as leading to P limitation. These data confirm the importance of P as an (and often the) important nutrient in controlling the degree of eutrophication in the river system. This pattern of high N:P ratio in pollutant sources exists in many other river systems including the Yangtze (Liu et al., 2018) and Ruhr (Westphal et al., 2020). Liu et al. (2018) identify the need to reduce agricultural fertilizer use and have better urban wastewater management in agreement with this study. However, often the reduction in total nutrient load into a river system can result in more extreme P limitation, as often the reduction in nutrient load (particularly from point source sewage treatment works) has been more effective in reducing P than N (Viaroli et al., 2018; Westphal et al., 2020). These results emphasize further the need for science-based management decisions if the problem of human-induced eutrophication in river systems is to be alleviated.

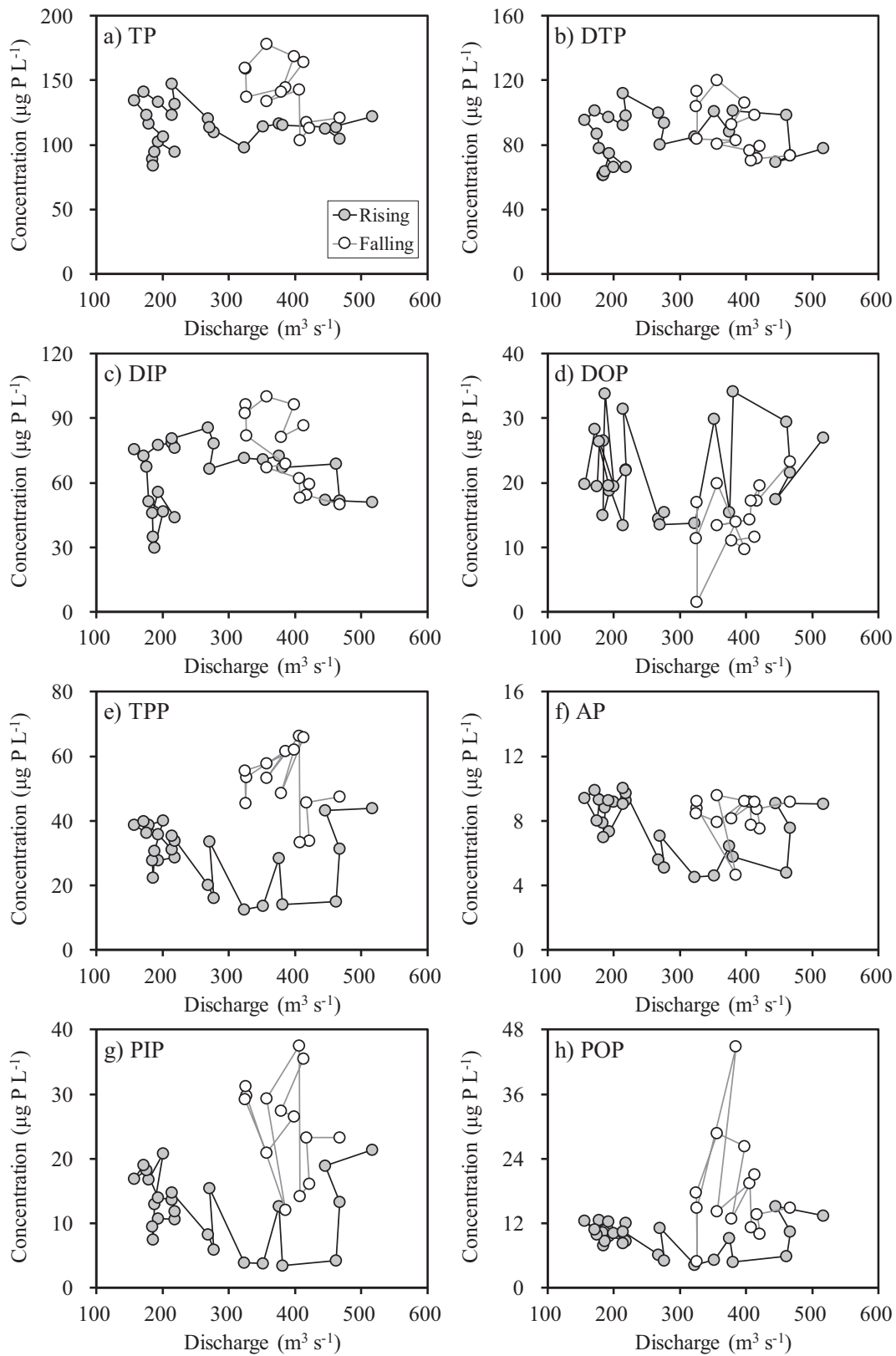


Fig. 8. Relationship between P species and discharge in the WJR sampling during a storm event (June 11–13, 2019).

5. Conclusions

In this study, the sampling of the whole Jiulong River system was carried out in both the wet and dry seasons to explore P speciation and cycling processes. Two major anthropogenic P sources (agriculture

waste and urban effluent) were characterized by detailed sampling from mainly single source subcatchments in the dry season. The Agriculture source (upper WJR) had the highest P concentration, which was mainly DIP from excess fertilizer being washed from the fields. In contrast, the West Urban source (sewage effluent in lower WJR) had a

Table 6

Summary of phosphorus fluxes and concentrations of the storm events at the exits from the North and West Jiulong River (NJR and WJR).

Items	Storm event	River	TP	DTP	DIP	DOP	TPP	AP	PIP	POP	Reference
P flux (kg P day ⁻¹)	2019.6	WJR	3482	2384	1905	478	1099	210	489	399	This study
	2019.6	NJR	10,162	5006	3914	1093	5156	623	2337	2196	This study
	2013.7	NJR	195,410	84,002	18,153	65,760	111,498	ND	ND	ND	Chen et al., 2015
EMC (µg P L ⁻¹)	2019.6	WJR	130.1	89.1	71.2	17.9	41.0	7.9	18.3	14.9	This study
	2019.6	NJR	87.6	45.0	34.1	10.9	42.7	5.3	19.4	17.9	This study
	2013.7	NJR	533	220	47	173	313	ND	ND	ND	Chen et al., 2015
Baseflow (µg P L ⁻¹)	2019.6	WJR	94.6	66.0	44.0	22.0	28.6	9.3	10.7	8.7	This study
	2019.6	NJR	69.9	42.3	29.9	12.4	27.6	4.1	13.7	9.8	This study
	2013.7	NJR	306	264	83	181	42	ND	ND	ND	Chen et al., 2015

Note: ND: not detected. EMC: event mean concentration. Baseflow is the measured concentration at the start of storm (refer to Figs. 5–6). Storm event in June 2019 was smaller in size than storm C, which occurred in July 2013 (refer to Chen et al. (2015)).

much higher proportion of organic P, both particulate (POP) and dissolved organic P (DOP). We observed a major transformation of P speciation in the reservoirs in the main NJR where total particulate P (TPP) and DIP decreased while POP increased due to increased sedimentation of P-rich particles and biological uptake causing a conversion from DIP to POP. All P species increased at the beginning of the storm, followed by a decrease on the rising hydrograph due to dilution. The final concentration of all P species was higher in the falling hydrograph than during baseflow, confirming that storms increase the flux of P out of the catchment. During the storm, P was initially washed off the fields while during the falling hydrograph P increased due to interflow and other longer-term sources. This research confirms the importance of human activities in the Jiulong River watershed, which have substantially altered P sources, cycling and export under baseflow and stormflow. Our data identifying and characterizing the major pollutant sources in the two branches of the Jiulong River are necessary if we are to develop science-based management schemes to control the harmful effects of increased P and the resultant eutrophication in the river system and the adjacent coastal area.

CRedit authorship contribution statement

Xin Yuan: Writing - original draft. **Michael Krom:** Writing - review & editing. **MingZhen Zhang:** Data curation. **Nengwang Chen:** Research design and writing.

Declaration of competing interest

None.

All authors have approved the manuscript and agree with its submission to Science of the Total Environment.

Acknowledgements

This research was supported by the National Natural Science Foundation of China (No. 51961125203; No. 41676098; No. 41376082). We thank Yan Fang and Qing Tian for their assistance with fieldwork. Special thanks are given to the Hydrological Station for providing hydrological data. This work was undertaken by Professor Krom during his visiting Professorship at Xiamen University, which due to the Covid-19 pandemic had to be carried out by virtual visits and not in person. He would like to dedicate his contribution to this work to his granddaughter River Yaniv Krom who was born on June 25th, 2020.

References

- Benitez-Nelson, C.R., 2000. The biogeochemical cycling of phosphorus in marine systems. *Earth Sci. Rev.* 51, 109–135.
- Bowes, M.J., House, W.A., Hodgkinson, R.A., Leach, D.V., 2005. Phosphorus-discharge hysteresis during storm events along a river catchment: the River Swale, UK. *Water Res.* 39, 751–762.
- Chen, N., Wu, J., Hong, H., 2012. Effect of storm events on riverine nitrogen dynamics in a subtropical watershed, southeastern China. *Sci. Total Environ.* 431, 357–365.
- Chen, N., Wu, Y., Chen, Z., Hong, H., 2015. Phosphorus export during storm events from a human perturbed watershed, southeast China: implications for coastal ecology. *Estuar. Coast. Shelf Sci.* 166, 178–188.
- Chen, N., Hong, H., Gao, X., 2018a. Securing drinking water resources for a coastal city under global change: scientific and institutional perspectives. *Ocean Coast. Manag.* 104427.
- Chen, Y.N., Chen, N.W., Li, Y., Hong, H.S., 2018b. Multi-timescale sediment responses across a human impacted river-estuary system. *J. Hydrol.* 560, 160–172.
- Correll, D.L., Jordan, T.E., Weller, D.E., 1999. Transport of nitrogen and phosphorus from Rhode River watersheds during storm events. *Water Resour. Res.* 35, 2513–2521.
- Dynesius, M., Nilsson, C., 1994. Fragmentation and flow regulation of river systems in the Northern third of the world. *Science* 266, 753–762.
- Eccles, R., Zhang, H., Hamilton, D., 2019. A review of the effects of climate change on riverine flooding in subtropical and tropical regions. *J. Water Clim. Change* 10, 687–707.

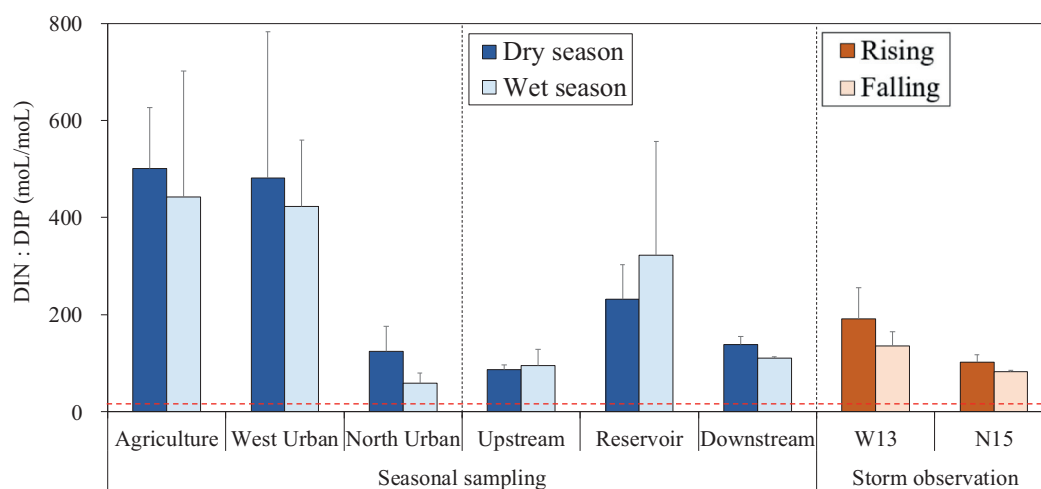


Fig. 9. The molar ratio of DIN:DIP among river sections during seasonal sampling and storm observation. Data are shown as mean with one standard deviation (SD) excluding outliers (>3SD). The red dotted line indicates the Redfield ratio of 16N:1P. (For interpretation of the references to color in this figure legend, the reader is referred to the web version of this article.)

- Elser, J.J., 2012. Phosphorus: a limiting nutrient for humanity? *Curr. Opin. Biotechnol.* 23, 833–838.
- Filippelli, G.M., 2008. The global phosphorus cycle: past, present, and future. *Elements* 4, 89–95.
- Gao, X.J., Chen, N.W., Yu, D., Wu, Y.Q., Huang, B.Q., 2018. Hydrological controls on nitrogen (ammonium versus nitrate) fluxes from river to coast in a subtropical region: observation and modeling. *J. Environ. Manag.* 213, 382–391.
- House, W.A., Warwick, M.S., 1998. Hysteresis of the solute concentration/discharge relationship in rivers during storms. *Water Res.* 32, 2279–2290.
- Kang, X., Song, J., Yuan, H., Shi, X., Yang, W., Li, X., et al., 2017. Phosphorus speciation and its bioavailability in sediments of the Jiaozhou Bay. *Estuar. Coast. Shelf Sci.* 188, 127–136.
- Lenes, J.M., Darrow, B.A., Walsh, J.J., Prospero, J.M., He, R., Weisberg, R.H., et al., 2008. Saharan dust and phosphatic fidelity: a three-dimensional biogeochemical model of *Trichodesmium* as a nutrient source for red tides on the West Florida Shelf. *Cont. Shelf Res.* 28, 1091–1115.
- Lin, J., Chen, N., Yuan, X., Tian, Q., Hu, A., Zheng, Y., 2020. Impacts of human disturbance on the biogeochemical nitrogen cycle in a subtropical river system revealed by nitrifier and denitrifier genes. *Sci. Total Environ.* 746, 141139.
- Liu, X.C., Beusen, A.H.W., Van Beek, L.P.H., Mogollon, J.M., Ran, X.B., Bouwman, A.F., 2018. Exploring spatiotemporal changes of the Yangtze River (Changjiang) nitrogen and phosphorus sources, retention and export to the East China Sea and Yellow Sea. *Water Res.* 142, 246–255.
- Lu, T., Chen, N., Duan, S., Chen, Z., Huang, B., 2016. Hydrological controls on cascade reservoirs regulating phosphorus retention and downriver fluxes. *Environ. Sci. Pollut. Res.* 23, 24166–24177.
- Lu, W.W., Lei, H.M., Yang, D.W., Tang, L.H., Miao, Q.H., 2018. Quantifying the impacts of small dam construction on hydrological alterations in the Jiulong River basin of Southeast China. *J. Hydrol.* 567, 382–392.
- Maavara, T., Parsons, C.T., Ridenour, C., Stojanovic, S., Duerr, H.H., Powley, H.R., et al., 2015. Global phosphorus retention by river damming. *Proc. Natl. Acad. Sci. U. S. A.* 112, 15603–15608.
- Maavara, T., Akbarzadeh, Z., Van Cappellen, P., 2020. Global dam-driven changes to riverine N:P:Si ratios delivered to the coastal ocean. *Geophys. Res. Lett.* 47.
- Maberly, S.C., King, L., Dent, M.M., Jones, R.I., Gibson, C.E., 2002. Nutrient limitation of phytoplankton and periphyton growth in upland lakes. *Freshw. Biol.* 47, 2136–2152.
- Mok, J.-S., Kim, S.-H., Kim, J., Cho, H., An, S.-U., Choi, A., et al., 2019. Impacts of typhoon-induced heavy rainfalls and resultant freshwater runoff on the partitioning of organic carbon oxidation and nutrient dynamics in the intertidal sediments of the Han River estuary, Yellow Sea. *Sci. Total Environ.* 691, 858–867.
- Niyogi, D.K., Koren, M., Arbuckle, C.J., Townsend, C.R., 2007. Stream communities along a catchment land-use gradient: subsidy-stress responses to pastoral development. *Environ. Manag.* 39, 213–225.
- Paerl, H.W., 2006. Assessing and managing nutrient-enhanced eutrophication in estuarine and coastal waters: interactive effects of human and climatic perturbations. *Ecol. Eng.* 26, 40–54.
- Perrone, J., Madramootoo, C.A., 1998. Improved curve number selection for runoff prediction. *Can. J. Civ. Eng.* 25, 728–734.
- Reinhard, C.T., Planavsky, N.J., Gill, B.C., Ozaki, K., Robbins, L.J., Lyons, T.W., et al., 2017. Evolution of the global phosphorus cycle. *Nature* 541, 386–389.
- River, M., Richardson, C.J., 2018. Particle size distribution predicts particulate phosphorus removal. *Ambio* 47, 124–133.
- Schoumans, O.F., Chardon, W.J., Bechmann, M.E., Gascuel-Oudou, C., Hofman, G., Kronvang, B., et al., 2014. Mitigation options to reduce phosphorus losses from the agricultural sector and improve surface water quality: a review. *Sci. Total Environ.* 468, 1255–1266.
- Seitzinger, S.P., Mayorga, E., Bouwman, A.F., Kroeze, C., Beusen, A.H.W., Billen, G., et al., 2010. Global river nutrient export: a scenario analysis of past and future trends. *Glob. Biogeochem. Cycles* 24.
- Slomp, C.P., 2011. 5.06 - phosphorus cycling in the estuarine and coastal zones: sources, sinks, and transformations. In: Wolanski, E., McLusky, D. (Eds.), *Treatise on Estuarine and Coastal Science*. Academic Press, Waltham, pp. 201–229.
- Tilman, D., 1999. Global environmental impacts of agricultural expansion: the need for sustainable and efficient practices. *Proc. Natl. Acad. Sci. U. S. A.* 96, 5995–6000.
- Treguer, P., Nelson, D.M., Vanbennekum, A.J., Demaster, D.J., Leynaert, A., Queguiner, B., 1995. The silica balance in the world ocean: a reestimate. *Science* 268, 375–379.
- Van Drecht, G., Bouwman, A.F., Harrison, J., Knoop, J.M., 2009. Global nitrogen and phosphate in urban wastewater for the period 1970 to 2050. *Glob. Biogeochem. Cycles* 23.
- Viaroli, P., Soana, E., Pecora, S., Laini, A., Naldi, M., Fano, E.A., et al., 2018. Space and time variations of watershed N and P budgets and their relationships with reactive N and P loadings in a heavily impacted river basin (Po river, Northern Italy). *Sci. Total Environ.* 639, 1574–1587.
- Wei, J.-F., Chen, H., Liu, Y.-L., Shan, K., Yao, Q., He, H.-J., et al., 2011. Phosphorus forms of the suspended particulate matter in the Yellow River downstream during water and sediment regulation 2008. *Environ. Sci.* 32, 368–374.
- Westphal, K., Musolf, A., Graeber, D., Borchardt, D., 2020. Controls of point and diffuse sources lowered riverine nutrient concentrations asynchronously, thereby warping molar N:P ratios. *Environ. Res. Lett.* 15.
- Withers, P.J.A., Jarvie, H.P., 2008. Delivery and cycling of phosphorus in rivers: a review. *Sci. Total Environ.* 400, 379–395.
- Yu, D., Yan, W., Chen, N., Peng, B., Hong, H., Zhuo, G., 2015. Modeling increased riverine nitrogen export: source tracking and integrated watershed-coast management. *Mar. Pollut. Bull.* 101, 642–652.
- Zimmer, M.A., Lautz, L.K., 2014. Temporal and spatial response of hyporheic zone geochemistry to a storm event. *Hydrol. Process.* 28, 2324–2337.
- Zuijgeest, A., Wehrli, B., 2017. Carbon and nutrient fluxes from floodplains and reservoirs in the Zambezi basin. *Chem. Geol.* 467, 1–11.